NASA TECHNICAL NOTE

NASA TN D-6779

NASA TN D-6779

AN ELECTROCHEMICAL MODEL FOR HOT-SALT STRESS-CORROSION OF TITANIUM ALLOYS

by Marvin Garfinkle

Lewis Research Center
Cleveland, Ohio 44135

NATIONAL AERONAUTICS AND SPACE ADMINISTRATION • WASHINGTON, D. C. • APRIL 1972

1. Report No. NASA TN D-6779	2. Government Accession No.	3. Recipient's Catalog No.
4. Title and Subtitle AN ELECTROCHEMICAL MODEL FOR HOT-SALT STRESS-CORROSION OF TITANIUM ALLOYS		5. Report Date April 1972
		6. Performing Organization Code
7. Author(s) Marvin Garfinkle		8. Performing Organization Report No. E-6456
		10. Work Unit No. 134-03
9. Performing Organization Name and Address Lewis Research Center National Aeronautics and Space Administration Cleveland, Ohio 44135		11. Contract or Grant No.
		13. Type of Report and Period Covered Technical Note
12. Sponsoring Agency Name and Address National Aeronautics and Space Administration Washington, D. C. 20546		14. Sponsoring Agency Code
15. Supplementary Notes		

16. Abstract

An electrochemical model of hot-salt stress-corrosion cracking of titanium alloys is proposed based on an oxygen-concentration cell. Hydrogen embrittlement is proposed as the direct cause of cracking, the hydrogen being generated as the result of the hydrolysis of complex halides formed at the shielded anode of the electrochemical cell. The model was found to be consistent with the diverse observations made both in this study and by many investigators in this field.

17. Key Words (Suggested by Author(s)) Stress corrosion Titanium alloys Hydrogen embrittlement	18. Distribution Statement Unclassified - unlimited

19. Security Classif. (of this report) Unclassified	20. Security Classif. (of this page) Unclassified	21. No. of Pages 38	22. Price* $3.00

* For sale by the National Technical Information Service, Springfield, Virginia 22151

CONTENTS

AN ELECTROCHEMICAL MODEL FOR HOT-SALT STRESS-CORROSION OF TITANIUM ALLOYS

by Marvin Garfinkle

Lewis Research Center

SUMMARY

An electrochemical model of hot-salt stress-corrosion cracking of titanium alloys is proposed to correlate the diverse observations made concerning this process. According to the model, an oxygen-concentration cell exists between the exposed surface of the corrosion specimen and shielded areas, such as under salt crystals and at crack tips. Oxygen is reduced at the exposed cathode regions, while substrate dissolution occurs at the shielded anodes with the formation of complex halides. The hydrolysis of these halides is the source of hydrogen that subsequently embrittles the substrate.

The model is consistent with observations made concerning the distribution of various ions and absorbed hydrogen in the vicinity of stress-corrosion cracks. The model is also consistent with the effects of salt composition and various surface additives on the susceptibility to stress-corrosion cracking as well as the effects of alloying and coatings.

INTRODUCTION

In numerous laboratory experiments, titanium alloys commonly used in compressor components of turbine aircraft engines have been found to be susceptible to hot-salt stress-corrosion cracking. Service failures of such compressor components have been reported, but none could be conclusively related to stress-corrosion cracking (ref. 1). To resolve this discrepancy, extensive investigations of the mechanical and atmospheric conditions that lead to cracking of commercial alloys have been conducted (refs. 2 and 3). Apparently, the limiting conditions that lead to cracking have not been exceeded in present engines under normal operating conditions. However, because future engines will probably be operating at higher temperatures and stresses for prolonged periods of time, it is imperative that the processes responsible for stress-corrosion cracking in titanium alloys be identified.

The observation by previous investigators (refs. 2 and 3) that the substrate is embrittled as a result of the stress-corrosion process precludes simple dissolution as the failure mode and instead suggests that an embrittling species is generated by the corrosion process. It is now generally accepted that such is the case and that hydrogen embrittlement is the direct cause of cracking. Disagreement exists (refs. 4 to 6), however, as to the mechanism of hydrogen generation.

Hot-salt stress-corrosion cracking of titanium alloys appears to consist of four basic processes:

(1) Substrate corrosion
(2) Hydrogen generation
(3) Substrate embrittlement
(4) Crack initiation and propagation

The first two, which have been least examined, involve the chemistry of the salt, the atmosphere, and the substrate, while the last two, which have been extensively investigated, involve the physical and metallurgical properties of the substrate alone. Observations designed to elucidate the first two basic processes were of secondary importance in most metallurgical studies and therefore were usually not substantiated by critical experiments. Nevertheless, sufficient data have been gathered concerning the effects of atmosphere and salt composition on the stress-corrosion process for various models to have been proposed in the literature. These models can be divided into two classes. Models in the first class require direct salt-atmosphere-substrate interactions for the formation of the embrittling species, of which the Rideout pyrohydrolysis (RPH) model (ref. 4) is the most comprehensive. In the second class are models which assume that electrochemical processes are responsible for the generation of the embrittling species, such as the Ripling electrochemical (REC) model (ref. 5).

Pyrohydrolysis is an analytical technique devised for the determination of halogens in salts that readily hydrolyze. Steam is passed over the salt at elevated temperatures, and the effluent is analyzed for hydrogen halide. According to the RPH model, the pyrohydrolysis reaction takes the form

$$Ti + 2NaCl + 2H_2O \rightarrow TiCl_2 + 2NaOH + 2H \qquad (1)$$

The resulting titanium dichloride readily hydrolyzes at elevated temperature to form hydrogen chloride, which subsequently reacts with the substrate to form hydrogen and additional titanium dichloride. The hydrolysis reaction then repeats, beginning another hydrogen generation cycle.

In contrast to the pyrohydrolysis model, the REC model assumes that stress-corrosion cracking is an electrochemical process that involves an oxygen concentration cell. Oxygen is consumed at the cathode according to the following process:

$$4e^{-} + O_2 \rightarrow 2O^{=} \qquad (2)$$

At the anode, simple metal dissolution is assumed to occur. While Lingwall and Ripling (ref. 5) do propose that hydrogen embrittlement is the ultimate mode of failure, they do not illustrate the means by which hydrogen could be generated from an oxygen concentration cell.

The purpose of this study was to examine the effects of atmosphere and other variables on the processes involved in stress-corrosion cracking of titanium alloys in order to evaluate possible embrittlement models, including the RPH and the REC models.

A series of titanium alloy tensile specimens were salt coated and then exposed at elevated temperature to different environments while subjected to various deadweight loads. To determine whether a particular load and environment had caused embrittlement, the exposed specimens were then tensile tested at room temperature.

The results of the investigation were evaluated in terms of possible rate-controlling reactions and mechanisms of the corrosion process. Based on this information, a comprehensive model for hot-salt stress-corrosion cracking of titanium alloys is proposed.

Since hydrogen embrittlement is widely considered to be intrinsic to the mechanism of stress-corrosion cracking, particular attention was paid to possible mechanisms that result in hydrogen generation. The metallurgical aspects of stress-corrosion cracking, such as the effects of microstructure on hydrogen embrittlement, were not considered in this study.

EXPERIMENTAL PROCEDURE

Material

Sheet tensile specimens were fabricated from commercial titanium alloy Ti-811 (Ti-8Al-1Mo-1V, w/0) sheet stock 0.50 mm (0.02 in.) thick. The material was received in the mill-annealed condition (1060 K (1450° F), 18 hr; air cooled). The chemical analysis as reported by the supplier is given in table I. To increase the maximum stress level to which the specimens could be subjected, the sheet material was cold-rolled to 0.40 mm (0.016 in.). This raised the ultimate strength from 1000 to 1300 MN/m^2 (145 to 190 ksi). The elongation was about 10 percent. Tensile specimens were machined to the configuration shown in figure 1. Specimen exposures at temperatures up to 700 K (800° F) for 24 hours did not affect the tensile values. Several unalloyed tensile specimens fabricated from 0.50-mm (0.02-in.) annealed sheet cold rolled to

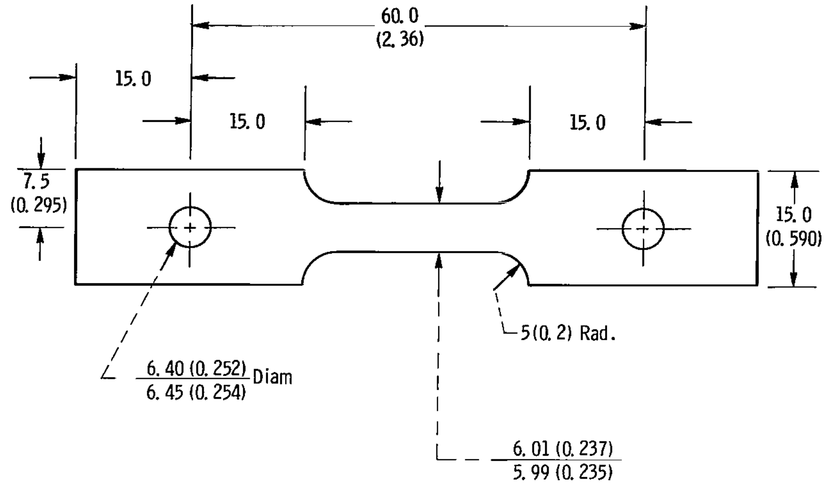

Figure 1. - Dimensional specifications for tensile specimens. Specimen thickness, 0.40 millimeter (0.016 in.).

0.40 mm (0.016 in.) with the configuration shown in figure 1 were also tested for reference purposes. Their ultimate strength was 876 MN/m^2 (127 ksi). Elevated temperature properties of both the alloyed and unalloyed tensile specimens are listed in table II.

Salting Procedure

Sodium chloride was deposited on the two faces of the reduced section of the sheet tensile specimens from a hot-air suspension at 525 K (485° F). The deposition was accomplished by clamping the specimen against the flat outside face of a rectangular window machined into the side of a 13-mm- (0.51-in.-) inner-diameter tube through which flowed a salt suspension in a hot air stream. The suspension was formed by injecting a saline aerosol into the hot air stream. The aerosol was created from a 1-percent sodium chloride solution in an apparatus described in detail by Gray and Johnston (ref. 7).

The salt deposited on the specimens was in the form of individual particles about 1 μm (40 μin.) in diameter. Because a complete coverage of the specimen surface would interfere with atmosphere-substrate reactions, a 75-percent salt coverage was arbitrarily chosen for this study. This coverage was equivalent to a salt concentration on the surface of approximately 0.032 mg/cm^2 (0.206 mg/in.^{2}).

Exposure and Evaluation Procedure

The test specimens were exposed to various atmospheres for 24 hours in a resistance-heated, stainless-steel, vertical-tube furnace (fig. 2). The specimens were deadweight loaded by external weights through a metal bellows arrangement.

Stress-corrosion exposures were made at temperatures of 625, 650, and 700 K (665°, 710°, and 800° F) in either nitrogen or oxygen environments. The bottle analyses of these gases are presented in table III. The gases were maintained at a room-temperature flow rate of 5 cm^3/s (6.5 ft^3/hr) throughout the test period and during heating and cooling. Their moisture content was controlled by liquid nitrogen trapping, by using the as-received gas, or by water bubbling at 273 or 295 K (32° or 71° F). These treatments resulted in estimated moisture contents of $<10^{-4}$, 10, 10^3, and $>10^4$ ppm, respectively.

The load train shown in figure 2 was introduced into the furnace only after the furnace had reached the desired temperature. A specimen reached furnace temperature

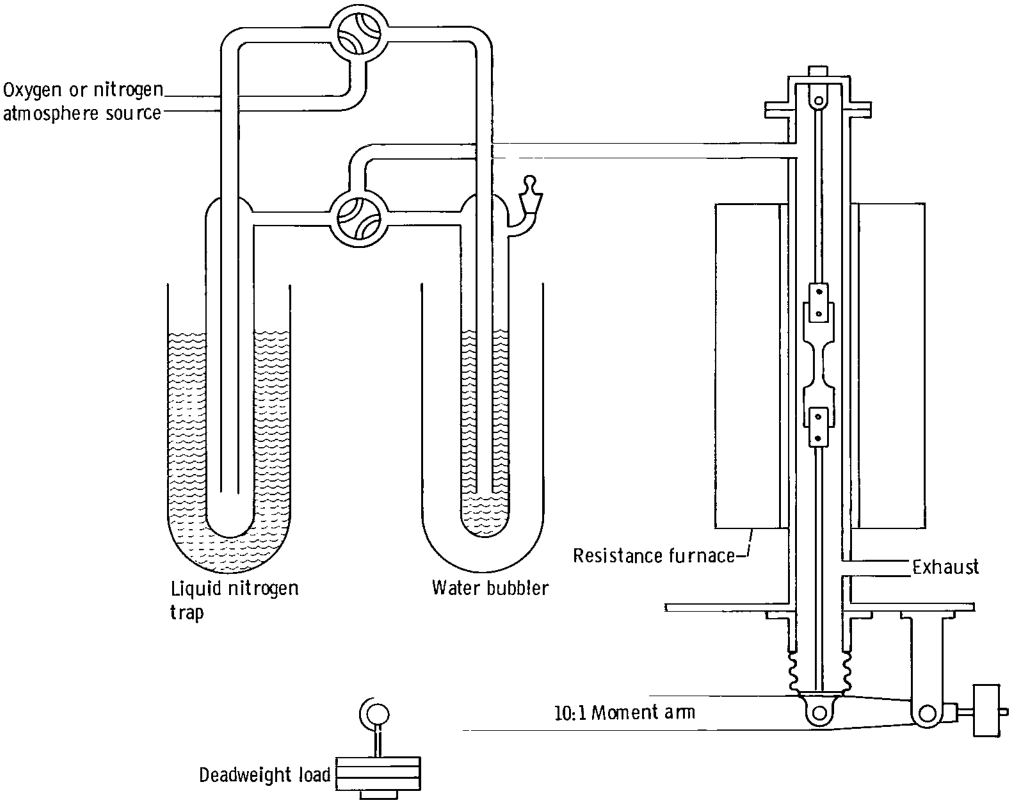

Figure 2. - Stress-corrosion exposure furnace with atmosphere source and loading apparatus.

in approximately 1/2 hour and was then deadweight loaded. After exposure, the specimens were unloaded and furnace cooled.

Room-temperature tensile testing of the exposed specimens for embrittlement evaluation was carried out at a crosshead speed of 0.042 mm/s (0.10 in./min).

Specimens that elongated less than that required to reach the ultimate strength, about 2 percent, were considered embrittled, as they could not accommodate the severe plastic deformation that accompanies necking. The deadweight load imposed on a salted specimen under a particular environment is reported as a percent of the maximum load sustained by an unsalted specimen under the same environmental conditions for the same duration and is denoted the percent rupture stress (%RS). The lowest percent rupture stress that results in embrittlement is denoted the brittle rupture stress and is a measure of the severity of the environment.

Special Procedures

Several tensile specimens were coated with various metals by vacuum deposition before salting. Coating thicknesses were limited to between 0.1 and 1.0 μm (4 to 40 μin.) so that they would not constitute a physical barrier to corrosion. The specimen edges were not coated.

To determine the effect of an impressed potential on the stress-corrosion process, an electrode arrangement was attached to the load train, as illustrated in figure 3. The thickness of each salt bridge was approximately 40 μm (1.6 mils). The resistance between electrodes depended on salt composition, temperature, and moisture content of the atmosphere. At a moisture level of $>10^4$ ppm water, the resistance was of the order of 20 MΩ for sodium chloride at 650 K (710° F) and about 400 kΩ for lithium chloride at 350 K (170° F).

RESULTS AND DISCUSSION

Current Models

Rideout pyrohydrolysis (RPH) model. - According to this model, nascent hydrogen is formed as a result of the stress-corrosion reaction, along with titanium dichloride and sodium hydroxide (reaction (1)). However, this reaction is thermodynamically unfavorable ($\Delta G^0 \approx +100$ kcal/mol) (refs. 8 and 9). Even if accelerators were present (ref. 10) or if the product of reaction (1) was assumed to be hydrogen gas instead of nascent hydrogen, any hydrogen chloride formed by the hydrolysis of titanium dichloride

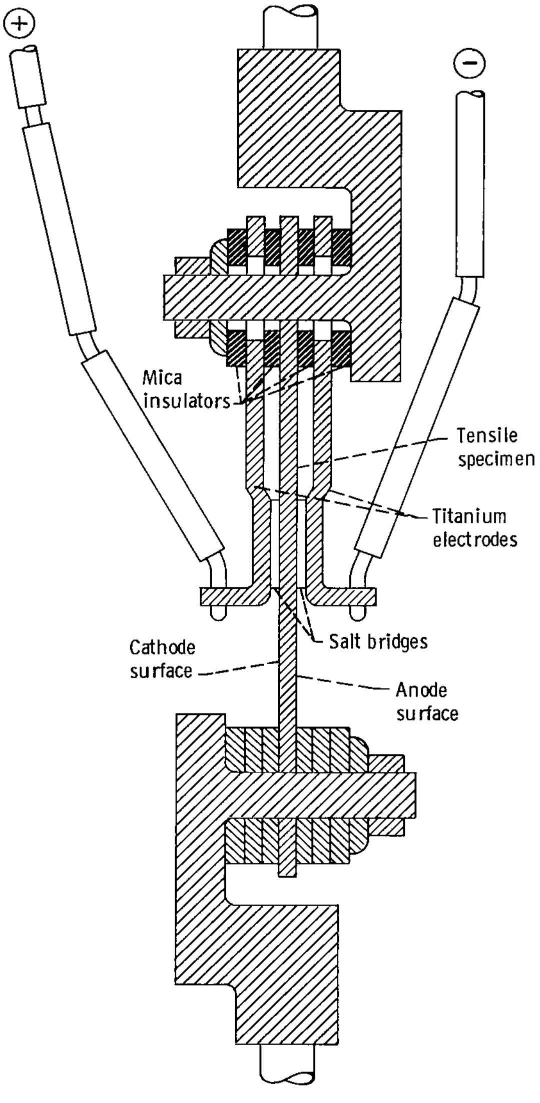

Figure 3. - Electrolytic corrosion cell for elevated-temperature stress-corrosion exposure.

would be neutralized by the sodium hydroxide present ($\Delta G^{o} \approx -30$ kcal/mol) (refs. 8 and 9) and would, therefore, not be available as an additional source of hydrogen, as required by the RPH model. Thus, it is highly unlikely that direct salt-atmosphere-substrate reactions play a significant role in stress-corrosion cracking. Nevertheless, the concept introduced by Rideout that the direct source of hydrogen is the result of a hydrolysis reaction has important ramifications that will be discussed in detail.

Ripling electrochemical (REC) model. - Three distinct observations support the oxygen-concentration cell concept proposed by the REC model for stress-corrosion cracking. The first observation is that pitting occurs only beneath a salt bead on a titanium alloy test specimen, the region most remote from the atmosphere (ref. 5). The second observation is that a potential develops between two titanium electrodes separated by a salt bridge when one is shielded from the atmosphere (ref. 5), the shielded electrode being anodic. The third observation is that an impressed potential between a stressed test specimen and an electrode separated from it by a salt bridge will significantly affect the time to failure, depending on the polarity of the test specimen. Unfortunately, the last observation led to contradictory results. According to Ripling et al. (ref. 11), an anodic specimen exhibits a time to failure greater than twice that of an unprotected specimen. However, according to Logan (ref. 6), it is a cathodic specimen that exhibits a time to failure greater than twice that of an unprotected specimen. The effect of an impressed potential on the time to failure was so significant in both of these experiments that this author can only conclude that one of the investigators cited had not properly identified the electrodes. Nevertheless, this evidence conclusively supports an electrochemical model for stress-corrosion cracking. Unfortunately, there is no plausible manner by which hydrogen could be formed by an oxygen-concentration cell, as is proposed by Ripling et al. (ref. 11).

The most elementary electrochemical process consists of an oxidation reaction at the anode and a reduction process at the cathode. In the case of simple electrolysis in an aqueous environment, these reactions might consist of metal dissolution at the anode and hydrogen formation at the cathode. In an oxygen-concentration cell, however, hydrogen discharge cannot occur, for at the anode oxidation is occurring and at the cathode oxygen is being reduced. Consequently, the REC model cannot explain the observed embrittlement associated with the stress-corrosion process.

Proposed Model

Neither the RPH nor the REC models are adequate to fully explain the processes occurring in stress-corrosion cracking of titanium alloys. In fact, these models are contradictory in that the RPH model requires a reducing environment for hydrogen generation while the REC model requires an oxidizing environment for the oxygen-concentration cell to operate. Nevertheless, the presence of hydrogen, whose source is a hydrolysis reaction in the RPH model, and the presence of an oxygen-concentration cell, as is proposed in the REC model, are in accordance with observations. Consequently, a hybrid model of stress-corrosion cracking in titanium alloys is proposed herein that incorporates features of both the RPH and the REC models.

The proposed model is electrochemical in nature; it assumes that ionic transport takes place through an adsorbed moisture layer on the surface of the substrate. As in the case of the REC model, it is assumed that an oxygen-concentration cell exists that results in oxygen being consumed at the cathode. Accordingly, the cathodic regions are those portions of the substrate exposed to the atmosphere. Anodic regions, unlike cathodic regions, are highly localized sites of rapid dissolution, such as grain boundaries, dislocation stress fields, and similar regions of high lattice strain. A crack tip, subjected to high lattice strains and shielded from the atmosphere, is very strongly anodic. At the anode it is assumed that the substrate oxidizes to a titanium halide. It is the hydrolysis of this species in a nonelectrochemical process, as in the case of the RPH model, that is the source of hydrogen ions that subsequently embrittles the substrate.

Cathode reactions. - Because the divalent oxygen ion is unstable in the presence of moisture, it is assumed in the proposed model that the reduction of oxygen at the cathode results in the formation of hydroxyl ions. The formation of hydroxyl ions is equivalent to the consumption of hydrogen ions. Accordingly, the cathode process can be represented by reaction (3).

$$4e^- + O_2 + 4H^+ \rightarrow 2H_2O \tag{3}$$

Hence, hydrogen ions are consumed at the cathode with the formation of water.

Anode reactions. - Titanium preferentially oxidizes to the trivalent state in chloride solutions under reducing conditions (ref. 12). However, the trivalent chloride tends to disproportionate at elevated temperatures (ref. 12) to the divalent and tetravalent chlorides. Thus, titanium chlorides of all three valences, or any one of them, could be present as a result of the stress corrosion process. Because tetravalent titanium corrosion products have been identified (ref. 13) on the surface of stress-corroded specimens along with little (ref. 14) or no divalent products (ref. 13), the tetravalent state will be used in illustrating the anode process. However, since all titanium chlorides tend to hydrolyze at elevated temperatures, the results would be similar in any case.

The tetravalent titanium ion cannot exist in contact with moisture, so it will be assumed that a complex ion (e.g., the hexachlorotitanate ion) forms as a result of the anode process:

$$Ti + 6Cl^- \rightarrow TiCl_6^= + 4e^- \qquad (4)$$

This complex ion readily hydrolyzes in contact with moisture (ref. 15). The hydrolysis process may involve more than a single step, with the oxychloride an intermediate product, as this species has been found in trace amounts as a corrosion product (ref. 16). The complete hydrolysis reaction can be represented as

$$TiCl_6^= + 2H_2O \rightarrow TiO_2 + 4H^+ + 6Cl^- \qquad (5)$$

where the hydrogen ions formed are the source of hydrogen for subsequent embrittlement.

Combining reactions (4) and (5) yields the overall anode process:

$$Ti + 2H_2O \rightarrow TiO_2 + 4H^+ + 4e^- \qquad (6)$$

Electrode half-cell potentials. - Quantitative thermodynamic data related to electrode half-cell reactions at elevated temperatures, particularly half-cell potentials, are generally unavailable. Fortunately, for the particular case of the electrode half-cell reactions involved in the proposed electrochemical model, half-cell potentials can be calculated, but only because the sole ion involved in these reactions is the hydrogen ion, whose free energy of formation is assumed zero in one molar solution.

The half-cell potentials were computed from standard free energies of formation data (refs. 8 and 9). Because the potentials are dependent on the hydrogen ion concentration of the electrolyte, they were corrected for a neutral solution, as would be the case at the onset of stress-corrosion. A pH of 6 is neutral, based on dissociation constant determinations made between 273 and 575 K (32° and 575° F) (ref. 17) and extrapolated to 650 K (710° F). The potentials are given in table IV. Under neutral conditions, the electromotive force of the proposed stress-corrosion reaction is approximately 2 volts, which is indicative of a thermodynamically favorable reaction.

The actual stress-corrosion process is so catastrophic that it can only be explained by reactions so thermodynamically favorable that competing reactions that might circumvent it are inconsequential. The overall stress-corrosion process can be represented in the proposed electrochemical model as the sum of the cathode and anode half-cell reactions that comprise it. Adding reactions (3) and (6) yields

$$Ti + O_2 \rightarrow TiO_2 \tag{7}$$

This process is thermodynamically more favorable than virtually any reaction that involves halides.

While halide compounds such as hydrogen chloride (ref. 18) are present as a result of stress-corrosion, according to the postulated electrochemical model they play an insignificant role in the processes that lead to the formation of the embrittling species. Other halides, such as complex titanium chlorides or oxychlorides, play an important but transient role in the anode process but they play no role in the overall electrode reactions listed in table IV.

Experiments and Observations

How well the proposed electrochemical model accounts for the diverse observations made by many investigators concerning stress-corrosion cracking was examined by comparison of model predictions both with results of experiments performed in this study and with results of other investigators.

Effect of atmospheric composition. - According to the proposed model, oxygen is consumed in the electrochemical corrosion process by reduction at the cathode, thus its absence should inhibit the stress-corrosion process. Oxygen could not be totally removed from the system, being adsorbed on the salt and substrate and dissolved in any moisture present. However, its effect on the stress-corrosion process can be tested by comparing the severity of attack under a nitrogen (low oxygen) atmosphere with that under an oxygen atmosphere. As predicted by the proposed model, oxygen did promote the stress-corrosion process (fig. 4 and table V).

The primary role of moisture in the proposed electrochemical model is to supply the embrittling species, hydrogen. A hydrogen concentration of 20 atom percent extending for a distance of 10 μm below the fracture surface is of the order of that found by Gray (ref. 19) in the vicinity of a corrosion crack. The amount of moisture required to produce this concentration of hydrogen in the restricted volume of a specimen of the configuration shown in figure 1 can be readily computed and is approximately 1 μg. Under the driest conditions observed, almost a magnitude greater amount of water is available. Thus, the amount of hydrogen required to embrittle the substrate is so minute that the loss of moisture by this process can be neglected in considering the stress-corrosion process as a whole. Nevertheless, this amount of moisture is all that is directly involved in the chemical processes of the proposed model.

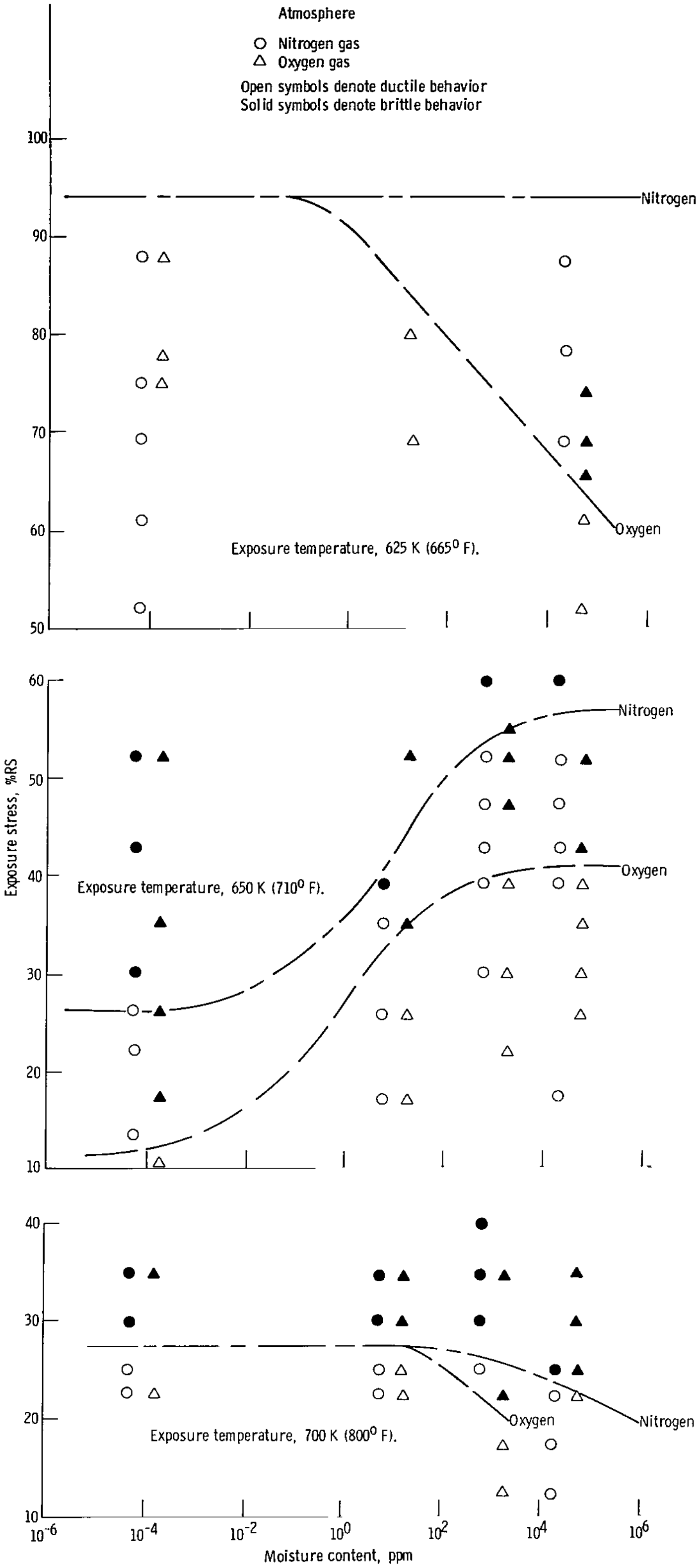

Figure 4. - Effect of atmosphere on stress-corrosion cracking of titanium alloy Ti-811 at various exposure temperatures. (Data from table V.)

Water, however, plays an important secondary role in that it does constitute the ionic transport medium, and thus is necessary for the initiation of the stress-corrosion process. Its source, moreover, need not be the atmosphere but instead could be water adsorbed on or entrained in the salt crystals. Thus, the role of moisture in the atmosphere may be overshadowed by the initial moisture present. In any case, water involved in ionic transport is not consumed in the overall electrochemical process, being formed at the cathode and consumed at the anode. Consequently, beyond that required to supply the embrittling species, it is not possible to predict by the proposed model alone the effect of atmospheric moisture on stress-corrosion cracking.

Effect of surface hydrogen ion concentration. - According to the proposed model, hydrogen ions are consumed at the cathode. Consequently, changing the surface pH should either promote or inhibit the cathode reaction. This predicted effect is illustrated in table IV. Lowering the surface pH should raise the cathode potential and should thereby promote the stress-corrosion process. This prediction could be readily tested by either acidulating the salt deposit or injecting a reactive gas such as hydrogen chloride into the gas stream. However, both techniques will corrode the titanium alloy surface. The latter technique will also cause cracking without the presence of salt (ref. 4), so that the results would be ambiguous. Instead, carbon dioxide was injected into the gas stream. Though only a mild acid former, the 10 percent carbon dioxide in the oxygen stream did reduce the rupture stress from 30 percent to 24 percent, as is shown in figure 5 and table VI, as predicted by the proposed model.

With hydrogen ions consumed at the cathode in accordance with the proposed model, raising the surface pH reduces the cathode potential and should thereby inhibit the stress-corrosion process. This effect can be illustrated by expressing the cathode reaction as

$$4e^- + O_2 + 2H_2O \rightarrow 4OH^- \qquad (8)$$

instead of reaction (3). This representation does not alter the basic reaction as hydrogen ion consumption is equivalent to hydroxyl ion formation. However, it does illustrate that the stress-corrosion process results in the formation of hydroxyl ions at the cathode and that the presence of an excess of hydroxyl ions should inhibit the electrode process. Accordingly, tensile specimens which had been salt coated in the manner previously described were wetted with a concentrated solution of sodium hydroxide in methanol. This solvent minimized any disturbance of the salt layer. As predicted by the proposed model, the presence of sodium hydroxide did raise the rupture stress, as is shown in figure 5 and table VI.

Hydrogen distribution due to corrosion processes. - According to the proposed model, hydrogen formation and absorption into a uniaxially loaded exposure specimen

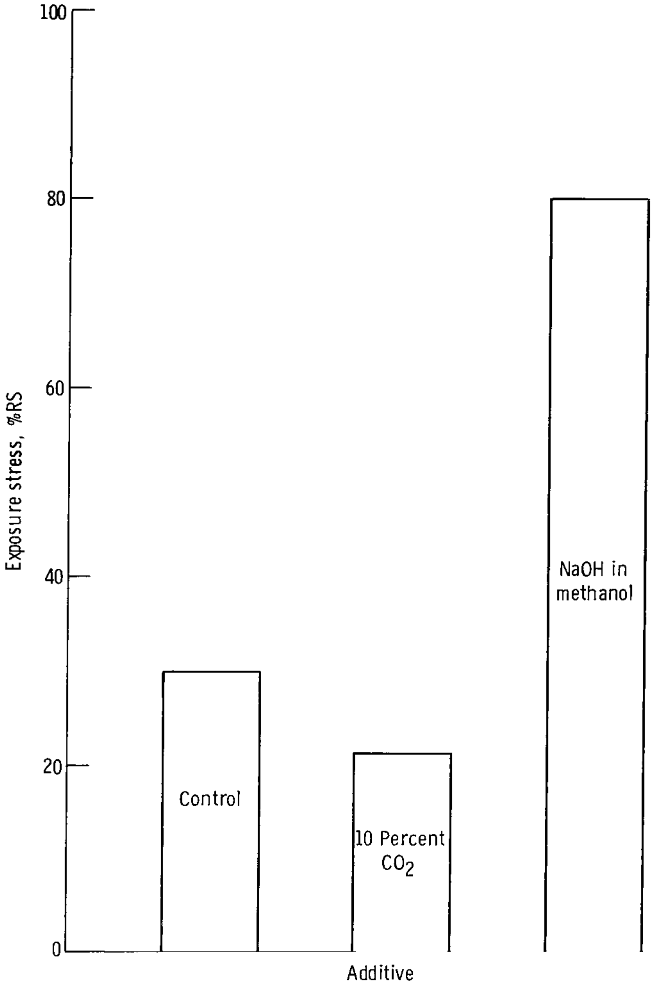

Figure 5. - Effect of specimen surface and atmosphere additives on stress-corrosion cracking at 650 K (710° F) in oxygen with a moisture content of 10 ppm. (Data from table VI.)

occurs at anodic sites shielded from the atmosphere, such as under salt crystals. The anode process results in corrosion pits in localized regions of high hydrogen concentration. Cracks are initiated at these triaxially stressed corrosion pits and propagate normal to the loading direction. Such cracks will propagate laterally, joining similar cracks, and into the metal, resulting in a crescent-shaped discontinuity as shown in the fractograph of figure 6(a). This figure is typical of the fractured surfaces of exposure specimens that failed in a brittle manner during room-temperature tensile testing. The crescent-shaped region is the stress-corrosion crack; its surface was discolored, indicating that it had formed while exposed to the furnace atmosphere. Figure 6(b) is a representation of the stress-corrosion crack with the anode and cathode regions specified.

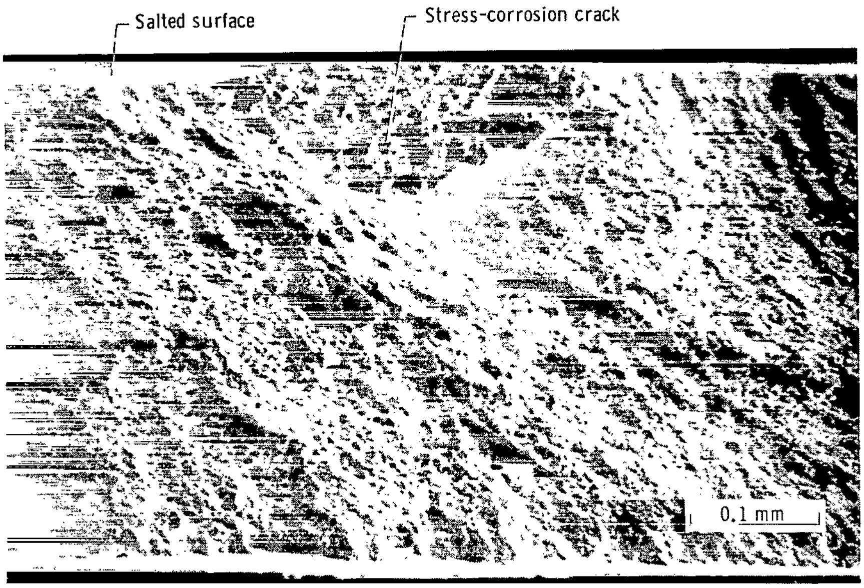

(a) SEM fractograph.

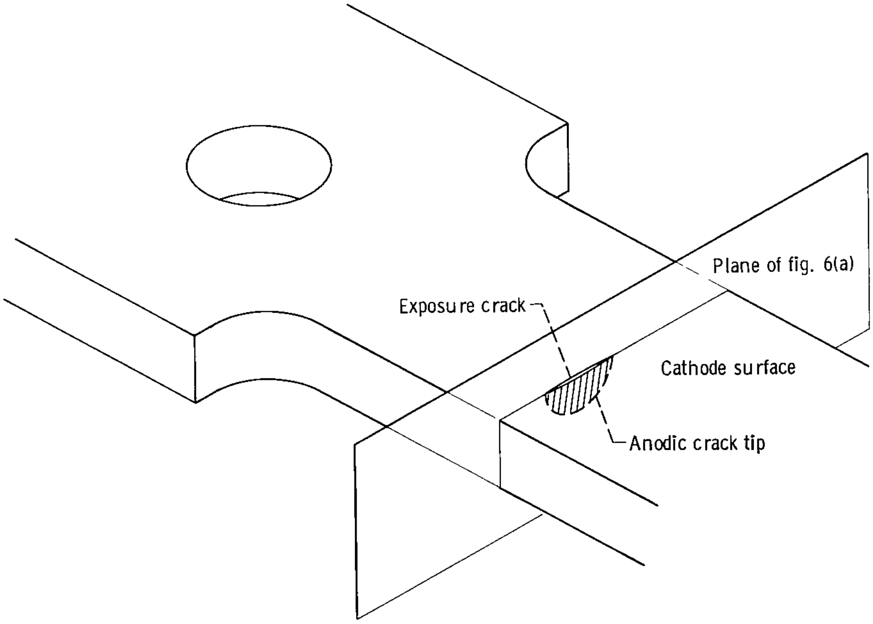

(b) Schematic diagram.

Figure 6. - Stress-corrosion tensile specimen with exposure crack and associated electrochemical cell.

Figure 7 illustrates schematically the crack initiation and propagation process according to the proposed model. Figure 7(a) illustrates a corrosion pit formed in a shielded area of the specimen surface. As a result of the anode process, the pit is surrounded by an embrittled region of high hydrogen concentration. When this concentration reaches a level sufficient to lower the fracture stress of this embrittled region below that of the triaxial stress field resulting from the applied load, cracking will occur. The crack resulting from the fracture of this embrittled layer will be blunted by plastic deformation in the ductile metal below, as is illustrated in figure 7(b), in which it is assumed that the substrate is an isotropic continuum. Adsorbed moisture from the surface will migrate to the crack tip, probably by capillarity, thereby reestablishing the anode. Hydrogen formed at the anode will embrittle the high elastic stress

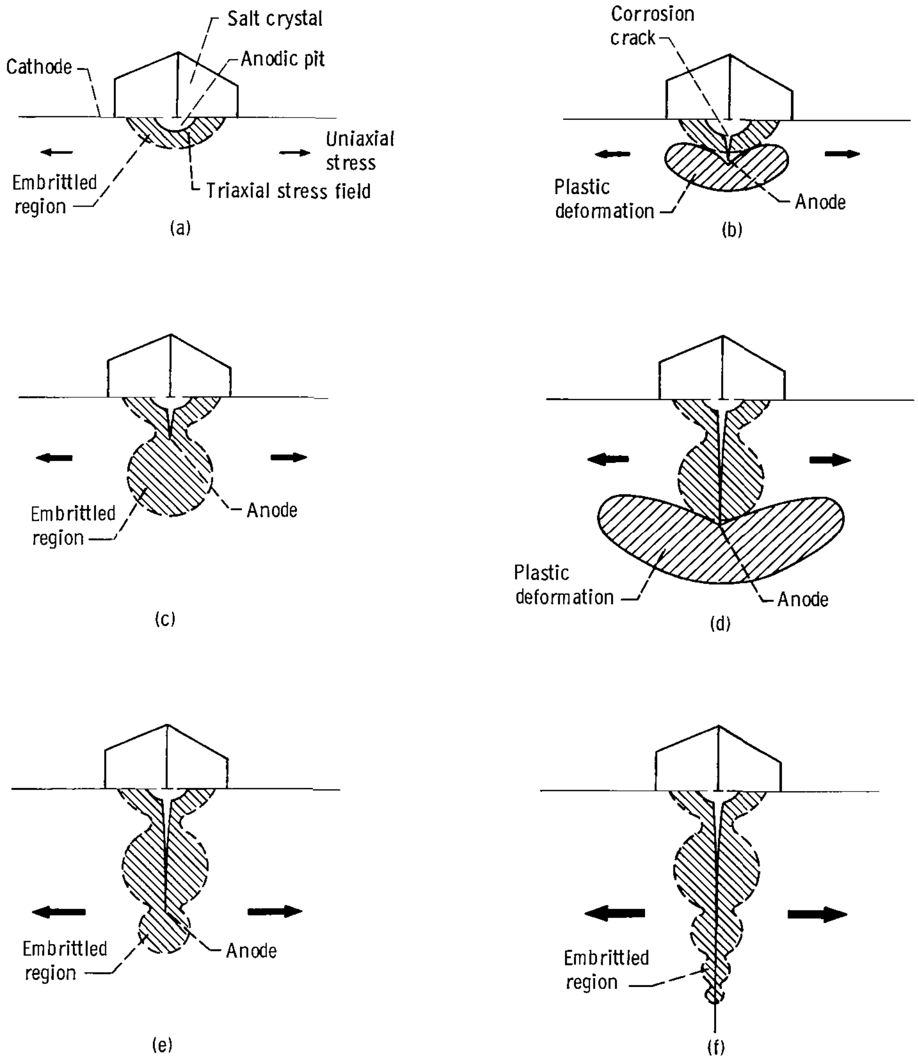

Figure 7. - Schematic representation of crack initiation and propagation leading to stress-corrosion failure.

field existing in advance of the crack tip (fig. 7(c)). When the concentration of absorbed hydrogen again reaches a level sufficient to lower the fracture stress of the embrittled region below that due to the applied load, the crack will again propagate to the ductile region below (fig. 7(d)). The sudden relaxation of the stress field in the embrittled region could cause the precipitation of hydride particles (ref. 20). Any such particles that formed subsequent to cracking would play a minor role in the propagation process.

Because the applied load is constant, the stress at the crack tip will increase with each propagation step as the cross-sectional area is decreased. This process repeats itself (fig. 7(e)) with increasing rapidity until the crack length is sufficient to permit propagation without the electrochemical nucleation process (fig. 7(f)). That highly localized concentrations of hydrogen can occur as a result of this process is supported by the findings of Oriani (ref. 21), who showed that the absorption of hydrogen generated at a crack tip is greatly accelerated by the presence of a tensile stress field in advance of the crack tip.

Thus, according to the proposed model, a concentration of hydrogen in the vicinity of a stress-corrosion crack would be the result of its localized generation and absorption and not as a result of its diffusion from a surface region. In fact, such long-range diffusion processes play no significant role in this model. The role of the applied load is solely to establish the high elastic stress field and to subsequently crack the embrittled region.

The localized generation of hydrogen is suggested by the experimental findings of Gray (refs. 19 and 22). By use of the ion-probe mass-spectrometer and Laser microprobe he found that the concentration of hydrogen in the vicinity of a corrosion crack was much greater than in the surrounding material. Hydrogen concentrations considerably greater than 1000 ppm were found within 0.1 mm of a crack as compared with the overall hydrogen content of approximately 100 ppm as determined by chemical analysis.

If the localized concentrations of hydrogen found by Gray were the result of direct salt-atmosphere-substrate interactions and not an electrochemical process, its diffusion from the surface to the crack tip would require a high surface concentration of hydrogen. Such was not found to be the case in this study or by others (refs. 5 and 19). It might be argued that the tensile stress field in advance of the crack tip could attract hydrogen preferentially from the surface so that the average hydrogen concentration of the substrate need not increase. However, the stress field on either side of the crack is zero normal to the crack and is in compression tangent to it (ref. 23) and therefore would not constitute a preferential diffusion path. With hydrogen generated at the tip, as is proposed in the electrochemical model, long-range migration is not required.

The proposed model can also explain the incubation period that has been observed before cracking (ref. 4). Before the first crack is nucleated, the high localized stress field that accelerates hydrogen absorption is absent. Therefore, the time to nucleate a crack is much greater than the time to propagate an existing crack. Moreover, as the applied load is constant, the stress is lowest initially. Thus, surface treatments, such as shot-peening, which impose a compressive stress of the surface should prolong the incubation period for crack initiation.

Effect of cyclic exposure on corrosion processes. - According to the proposed model, anodic generation of hydrogen results in highly localized concentrations of this embrittling species in the exposure specimen. As long as generation of hydrogen is more rapid than its diffusion away from the anodic region, the concentration of hydrogen will increase at these sites. If for any reason the generation process is interrupted or the diffusion process is enhanced, the regions of high hydrogen concentration will diminish. Subjecting stress-corrosion specimens to cyclic exposure of temperature or load should have such an effect, thereby increasing the time to failure as measured by total exposure time. If the temperature is cycled, the hydrogen generation process is interrupted, allowing diffusion processes to diminish the regions of high hydrogen concentration. If the applied load is cycled, the high tensile stress field existing at the base of corrosion pits or at crack tips is relaxed, as is the lattice dilation resulting from the stress field. Hydrogen concentrated at these sites by virtue of the lattice dilation (ref. 20) will rapidly diffuse upon its relaxation because of the resulting gradient in chemical potential energy. Thus, under cyclic exposure conditions, the useful life of the specimen should be indefinite if the time of exposure to temperature and load during each cycle is less than the time necessary for crack initiation under the conditions of temperature and stress imposed and if the time between exposures is sufficiently long to equilibrate the hydrogen dissolved in the specimen. Even if these conditions were not fully met, the shorter the exposure time during each cycle, the lower the probability for crack initiation, and the longer the time to failure. Increasing temperature, however, should diminish the effect of cyclic exposure on the time to failure. With increasing temperature, the rate of hydrogen generation is increased, so that the time to initiate a crack becomes shorter. Thus, to be effective in inhibiting the stress-corrosion process, the time at temperature for each cycle must be shortened. If not, the time to failure of a cyclically exposed specimen will approach that of a noncyclically exposed specimen with increasing temperature.

For the aforementioned reasons, cyclic exposure should have the same effect on rupture stress as it does on time to failure. For the same total exposure time, cyclic exposure should permit a significantly greater imposed load to be sustained. Thus, if the exposure time within each cycle is less than the time to initiate the first crack, and if the time between exposures is sufficient to permit the equilibration of the dissolved hydrogen, the rupture stress should approach that of an unsalted specimen.

Gray (ref. 24) showed that cycling temperature and load, together or individually, increased the brittle rupture or threshold stress of the Ti-811 tensile specimens for a constant exposure time as compared with noncyclic exposure. Piper and Fager (ref. 25) showed similar results for temperature cycling alone. Gray (ref. 24) also showed that the effect of cyclic exposure becomes less with increasing temperature. In reference 14, it was shown that the total exposure time to failure increases with shorter exposure periods for each cycle, which was also predicted by the model.

Effect of impressed potential on corrosion processes. - According to the proposed model, the embrittling species is formed in the vicinity of the anode. Consequently, if a potential is impressed across a sheet-metal tensile specimen in such a manner that the faces of the reduced section are of opposite polarity (fig. 3), stress-corrosion cracking should initiate on the anodic face.

A potential of 36 volts was impressed on a tensile specimen by means shown in figure 3, resulting in a current density of approximately 3 $\mu A/cm^2$ (20 $\mu A/in.^2$). The specimen was exposed and evaluated in the conventional manner. The test conditions and results are presented in table VII. The surface of the fracture was bright except for a band of deep blue discoloration extending in from the anode edge approximately 0.15 mm (0.006 in.). The discolored region was similar to the exposure cracks in a conventionally loaded specimen, the fracture surface of which is shown in figure 8(a),

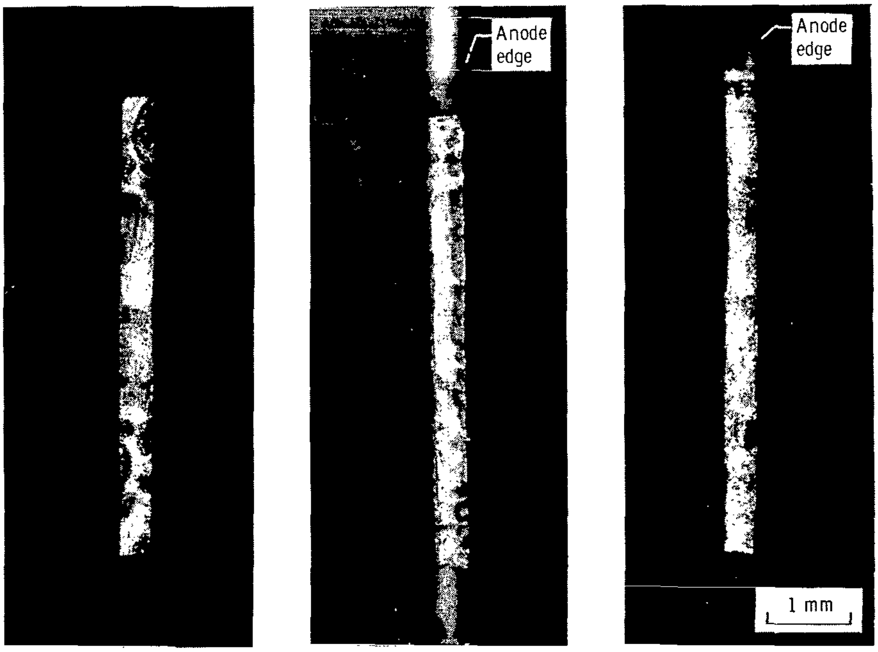

(a) Titanium alloy Ti-811 specimen exposed at 650 K (710° F).

(b) Titanium alloy Ti-811 specimen exposed at 650 K (710° F) with an impressed potential of 36 volts.

(c) Unalloyed titanium specimen exposed at 350 K (170° F) with an impressed potential of 72 volts.

Figure 8. - Fracture surfaces of stress-corrosion exposure specimens.

except that it was limited to the anodic edge of the fracture (fig. 8(b)), which indicated that stress-corrosion cracking had initiated at the anode as predicted by the proposed model. This observation is contrary to that found in electrolytic hydrogen charging from aqueous solutions (ref. 26), in which absorption occurs at the cathode.

Effect of alloy composition on corrosion processes. - According to the proposed model, the electrochemical reactions result in substrate corrosion and hydrogen generation. While titanium alloys are specified as the substrate, no particular alloy or composition is specified in the description of the electrochemical processes involved. Presumably, the corrosion and hydrogen generation process occurs regardless of minor changes in the composition of the alloy substrate. Thus, any differences in susceptibility to attack must be attributable to metallurgical factors, such as susceptibility to substrate embrittlement and resistance to crack initiation and propagation. This position is strongly supported by the findings of Gray (ref. 27), who reported that heat treatments that altered the microstructure had a very significant effect on susceptibility. Changes in the relative amounts of alpha and beta phases and their morphology in a particular alloy would affect not only its hydrogen diffusivity and solubility but its fracture toughness as well.

Virtually all titanium alloys contain aluminum, and attempts have been made to relate aluminum content to susceptibility to stress-corrosion cracking (refs. 28 and 29). As a result, the susceptibility of various alloys can be roughly categorized according to their aluminum content. According to the proposed model, however, aluminum content should not have a significant effect on the electrochemical processes. The chemistry of the trihalides of aluminum is surprisingly similar to that of the tetrahalides of titanium. With the exception of their respective fluorides, the halides of both titanium and aluminum are all highly susceptible to hydrolysis (ref. 30). In contrast, the hexafluoaluminate complex, like the hexafluotitanate complex, forms stable solids resistant to hydrolysis, even at stress-corrosion temperatures (refs. 12 and 30). Thus, the effect of aluminum content on susceptibility would be primarily related to metallurgical factors, and so would be greatly influenced by heat treatment. Gray (ref. 27) reported that the effect of heat treatment was far more significant than the effect of aluminum content on susceptibility.

Paradoxically, unalloyed titanium has not been found susceptible to hot-salt stress-corrosion cracking (ref. 31). This finding was confirmed in the present study. Salt-coated tensile specimens of unalloyed titanium with the configuration shown in figure 1 were subjected to stress levels up to 84 percent rupture stress under an oxygen atmosphere with 10 ppm moisture at 650 K (710° F). Embrittlement was not observed (table VIII). For comparison, a stress level of 25 percent rupture stress was sufficient to embrittle Ti-811 under these conditions.

Examination of unalloyed stress-corroded specimens revealed surface discoloration and pitting. It is apparent that the corrosion processes are similar to those involving alloys, which would be in accordance with the proposed model. Apparently, the corrosion processes that result in stress-corrosion cracking of titanium alloys are insufficient to cause hydrogen embrittlement of unalloyed titanium. Presumably, far greater amounts of hydrogen must be absorbed to cause embrittlement than can be produced by the electrochemical process.

The electrochemical process can be greatly accelerated by an impressed potential. Accordingly, an unalloyed tensile specimen was subjected to an impressed potential while under load in the apparatus shown in figure 3. For control purposes, the same conditions used in inducing stress corrosion cracking in the Ti-811 alloy were used (table VII). Even with a rupture stress of 75 percent, no loss in ductility was observed. However, by changing to a lithium chloride bridge and operating at 350 K (170° F) at a rupture stress of 75 percent, it was possible to crack unalloyed titanium (table IX). The bridge resistance was so reduced in comparison with sodium chloride, probably because lithium chloride is hygroscopic, that a current density of 0.3 mA/cm^2 (2 $mA/in.^2$) was possible at 72 volts. Even roughly relating absorbed hydrogen to current density, more than two magnitudes greater hydrogen absorption was required to crack the unalloyed specimen than that required to crack the Ti-811. The fracture surface was similar in appearance to that of the alloyed specimen, with a band of deep blue discoloration limited to the anode edge (fig. 8(c)). As predicted by the proposed model, the nature of corrosion reactions was not affected by the alloy elements present. It is more probable that differences in susceptibility arise primarily from metallurgical factors.

Effect of salt composition on corrosion processes. - According to the proposed model, it is not the physical properties of the salts themselves, such as ability to dissolve surface oxides (ref. 4), melting point (ref. 32), or aqueous solubility (ref. 32), that determine how severely they stress corrode the titanium alloys, but rather it is the properties of their constituent ions.

For the cathode reaction to occur, specifically reaction (8), free hydroxyl ions must be produced. Accordingly, the hydroxide of the salt cations must be soluble. Moreover, if a hydroxide precipitated, it could block the electrolytic conduction path.

For the hydrolysis process (reaction (5)) to occur, the titanium compound of the salt anion formed by the anode process (reaction (4)) must be susceptible to hydrolysis.

It is constructive to now examine the effect on stress-corrosion cracking of the salts studied in terms of these two criteria. According to the electrochemical model, the severity of attack will increase with increasing solubility of the hydroxide of the salt cation and with increasing susceptibility to hydrolysis of the titanium compound of the salt anion. The hydroxides of the alkali metals sodium and potassium have solubilities almost three magnitudes greater than those of the alkaline earth metals magnesium and calcium. While these data are for aqueous solutions (ref. 33), the relative solubilities should not change greatly for an adsorbed layer of water. Studies have shown that the alkali metal salts attack titanium alloys more severely than do alkaline earth metal salts (ref. 32).

The titanium salts most susceptible to hydrolysis are those involving halide anions (ref. 34). However, fluoride salts, particularly salts of the hexafluotitanate complex, are very stable and are not susceptible to hydrolysis (ref. 34). Studies (refs. 10 and 14) have shown that the chlorides, bromides, and iodides of the alkali metals are very effective in inducing stress-corrosion cracking in titanium alloys. The fluorides, however, are not very effective (ref. 35), as predicted by the proposed model.

The proposed electrochemical model also explains why extensive surface pitting and corrosion can occur without stress-corrosion cracking. The electrolytic processes responsible for pitting and general corrosion are independent of the hydrolysis reaction, the end result of the latter being the formation of the embrittling species.

The notable exceptions to the aforementioned criteria concern CuCl and hydrated $SnCl_2$. The cations of neither of them form soluble hydroxides, but both severely crack titanium alloys (ref. 10). Significantly, both salt cations are those of metals electronegative relative to titanium (ref. 36). As such, titanium should displace these metals from their salts. Such a process alleviates the need for an electrochemical mechanism for the formation of a species susceptible to hydrolysis.

That such displacement reactions do occur was shown by Rideout et al. (ref. 10), who reported the formation of metallic tin deposits on the surface of a $SnCl_2$ - coated titanium alloy specimen after stress-corrosion exposure.

Distribution of salt ions due to corrosion processes. - According to the proposed model, ion migration occurs within an adsorbed moisture layer between the mouth of a crack and the crack tip within the electrochemical cell. Consequently, salt cations such as sodium ions would tend to migrate towards the cathodic crack mouth, while salt anions such as chloride ions would tend to migrate towards the anodic crack tip. However, since both the cations and the anions originate at the salt-deposited surface, sodium ions would be expected to concentrate at the crack mouth, while the concentration of chloride ions would extend into the crack.

Rideout et al. (ref. 10), observed that the distribution of sodium ions in stress-corrosion cracks differed from that of chloride ions, as predicted by the proposed model, with the sodium ions concentrated at the crack mouth and the chloride ion concentration extending into the crack.

Electrochemical effects of surface deposits. - According to the proposed model, metallic deposits on the specimen surface could affect the susceptibility to stress-corrosion cracking. The deposit could either promote or inhibit the corrosion process, depending on its electronegativity relative to the titanium alloy substrate. For example, a deposit more electronegative than the substrate would be cathodic relative to the substrate and would, therefore, tend to promote the formation of anodic regions in the substrate, leading to accelerated corrosion. However, in the particular case of the stress-corrosion process, the effect of a cathodic surface deposit would probably not significantly increase the corrosion rate, as the surface is already cathodic by virtue of the oxygen-concentration cell.

A surface deposit less electronegative than the substrate would be anodic relative to the substrate and would, therefore, tend to corrode in preference to the substrate. Such a reaction would inhibit the stress-corrosion process, for only oxygen reduction would occur at the substrate. However, if the sacrificial corrosion of the surface deposit resulted in the formation of corrosion products susceptible to hydrolysis, the substrate could still be embrittled by the subsequent formation of hydrogen.

To determine whether the predicted effects of surface deposits are observed, tensile specimens were coated with palladium, aluminum, and magnesium films, by vapor deposition. They were then salted and tested in the same manner as were the uncoated specimens. Palladium is more electronegative than titanium (ref. 36) and should have, therefore, only a minor effect on susceptibility. Both aluminum and magnesium are less electronegative than titanium (ref. 36) and would be expected to inhibit substrate corrosion by anodic protection (table X). However, aluminum forms halide salts highly susceptible to hydrolysis and could, therefore, promote the stress-corrosion process.

Figure 9 and table XI show the effects of metallic surface deposits on the susceptibility to stress-corrosion cracking. The effect of palladium on susceptibility was minor, though it did increase the rupture stress, probably because the palladium constitutes a

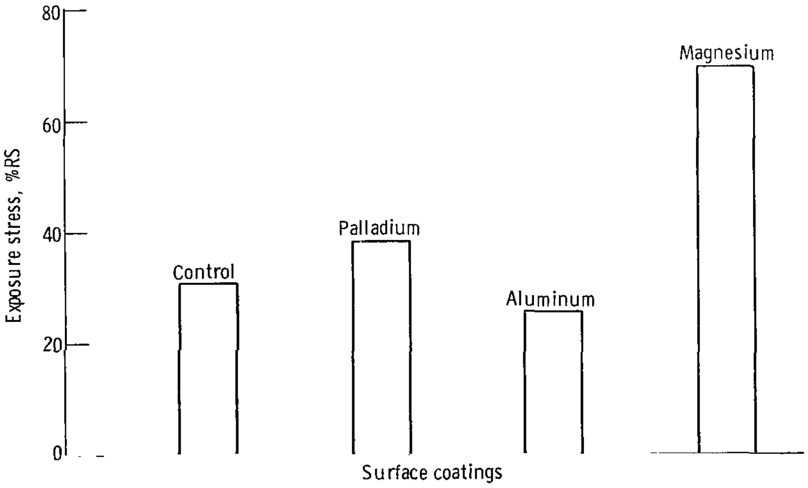

Figure 9. - Effect of metallic surface coating on stress-corrosion cracking of titanium alloy Ti-811 at 650 K (710° F) in oxygen with a moisture content of 10 ppm. (Data from table XI.)

barrier to corrosion. Aluminum, though less electronegative than the substrate, promoted the stress-corrosion process, while magnesium, also less electronegative than the substrate, inhibited stress-corrosion cracking, as predicted by the proposed model. Zinc, which is similar to magnesium, in that it is less electronegative than the substrate and forms stable chlorides, has been observed (ref. 18) to inhibit stress-corrosion cracking, even when scratched. This further indicates the electrochemical nature of the protection.

Practical Considerations

The useful life of a titanium alloy component in a critical application at elevated temperatures is limited by creep considerations, which apparently limit the imposed load to levels below the threshold for stress-corrosion cracking. However, as stronger titanium alloys with greater creep resistance are developed, the stress to initiate cracking during the design life of the part can become the load-limiting factor.

Creep-limited service failure, in which excessive creep of a component occurs beyond that for which it was designed, might only be an inconvenience or even require shut-down of the device involved. In contrast, crack-limited service failure of a component could be catastrophic. Thus, the useful life of a component in such service must be less than that for which a reasonable probability exists for crack initiation. So that the useful life is of a practical duration, either the load imposed must be conservative or the time for crack initiation must be maximized. Because the alloy itself is usually specified for its strength or strength/density ratio, the most advantageous course is to maximize the time for crack initiation. Two metallurgical variables known to increase the time for crack initiation are heat treating and shot-peening of existing alloys. Four possible chemical variables are considered in the following sections.

Effect of alloy composition. - Few alloys that have been formulated for corrosion resistance also show good high-temperature strength. Often the alloy elements that promote strength also decrease corrosion resistance, such as aluminum in titanium alloys. Thus, altering an alloy to significantly decrease susceptibility to stress-corrosion cracking can result in a significant sacrifice in strength. Increased life could just as well be achieved by limiting the load imposed on an existing alloy.

Effect of environment. - Experiments have shown that the salt composition or additives to the salt or atmosphere can significantly decrease the susceptibility of an alloy to stress-corrosion cracking. However, in most cases the environment itself determines the composition of the salt deposited, and the addition of chemicals to the salt or atmosphere during an extended useful life would probably be commercially prohibitive in a practical application because of allowable weight and volume limits.

Effect of surface protection. - To be reasonably practical, a coating to protect the substrate must remain protective for some reasonable time after rupture. To be competitive, the substrate must not degrade in any significant amount after coating rupture, so that it may be recoated without loss of useful life. However, in critical applications, coatings are rarely used to extend the life of corrosion-susceptible alloys to practical limits. Instead, in such applications, coatings are used to extend the life of alloys that have shown practical useful lives under the imposed loads without coatings.

Effect of exposure schedule. - While cyclic exposure can significantly decrease the susceptibility of an alloy, the exposure schedule is invariably dictated by the application. While minor changes in the schedule of exposure could probably be accommodated in many applications, it is doubtful whether such a course would be followed in a critical application to significantly extend the useful life.

As mentioned previously, of the two alternative means presented to extend the useful life of a component exposed to stress corrosion conditions, lengthening the time for crack initiation is more advantageous than limiting the imposed load. After consideration of the means available, however, limiting the imposed load may be the only one practical. While not strictly protection as defined previously, removal of accumulated salt deposits by an alkaline wash between exposure periods could be beneficial. Any residual alkaline deposit would tend to inhibit the cathode process, thus prolonging service life.

CONCLUDING REMARKS

The proposed electrochemical model of hot-salt stress-corrosion cracking in titanium alloys can account for the paradoxical observation of hydrogen embrittlement in an oxidizing atmosphere. According to the model, the atmosphere provides the oxygen-concentration cell responsible for the electrochemical process. The result is the formation of cathodic regions on the surface of the alloy where the reduction of oxygen occurs. At anode sites, regions shielded from the atmosphere, oxidation of the substrate to complex ions occurs. It is the hydrolysis of these complex ions at corrosion pits and at a crack tip that supplies the embrittling species.

In assuming that the generation of hydrogen occurs at the site of embrittlement, long-range diffusion processes are not required to allow highly localized concentrations of hydrogen to exist. Though the concentration of hydrogen is high at sites of incipient cracking (up to two magnitudes greater than the bulk hydrogen concentration), the volume occupied is very limited, so that only minute amounts of hydrogen are required to cause embrittlement.

Because sites of high hydrogen concentration are thermodynamically unstable, they exist only when the rate of hydrogen generation exceeds the rate of hydrogen diffusion. Thus, any condition that interrupts the generation or promotes the diffusion of hydrogen will decrease the susceptibility of an alloy to stress-corrosion cracking.

The following observations concerning stress-corrosion cracking have been examined with reference to the electrochemical model:

1. Hydrogen distribution adjacent to the fracture zone.
2. The distribution of cations and anions in stress-corrosion cracks.
3. The relative effect of various salts on the susceptibility to stress-corrosion cracking.
4. Relative susceptibility to stress-corrosion cracking of alloyed and unalloyed titanium.
5. The effect of acidic and alkaline surface additives on the susceptibility to stress-corrosion cracking.
6. The effect of cyclic exposure conditions on susceptibility to stress-corrosion cracking.
7. The effect of metallic coatings on the susceptibility to stress-corrosion cracking.

The model proposed is consistent with these observations.

Lewis Research Center,
National Aeronautics and Space Administration,
Cleveland, Ohio, February 2, 1972,
134-03.

REFERENCES

1. Ashbrook, Richard L.: A Survey of Salt Deposits in Compressors of Flight Gas Turbine Engines. NASA TN D-4999, 1969.

2. Anon.: Stress-Corrosion Cracking of Titanium. Spec. Tech. Publ. No. 397, ASTM, 1966.

3. Staehle, R. W.; Forty, A. J.; and van Rooyen, D., eds.: Fundamental Aspects of Stress Corrosion Cracking. Nat. Assoc. Corrosion Eng., 1969.

4. Rideout, S. P.; Louthan, M. R., Jr.; and Selby, C. L.: Basic Mechanisms of Stress-Corrosion Cracking of Titanium. Stress-Corrosion Cracking of Titanium. Spec. Tech. Publ. No. 397, ASTM, 1966, pp. 137-151.

5. Lingwall, R. G.; and Ripling, E. J.: Elevated Temperature Stress Corrosion of High Strength Sheet Materials in the Presence of Stress Concentrators. Materials Research Lab., Inc. (NASA CR-88979), Aug. 1967.

6. Logan, Hugh L.: The Mechanisms of Stress Corrosion of the Titanium Alloy Ti 8-1-1 Exposed to Salt Environments at Elevated Temperatures. Rep. 9468, National Bureau of Standards (NASA CR-82511), May 4, 1964.

7. Gray, Hugh R.; and Johnston, James R.: Hot-Salt Stress-Corrosion of a Titanium Alloy Under a Simulated Turbine-Engine Compressor Environment. NASA TN D-5510, 1969.

8. Boyd, W. K.; and Fink, F. W.: The Phenomenon of Hot-Salt Stress-Corrosion Cracking of Titanium Alloys. NASA CR-117, 1964.

9. Wicks, C. E.; and Block, F. E.: Thermodynamic Properties of 65 Elements - Their Oxides, Halides, Carbides, and Nitrides. Bulletin 605, Bureau of Mines, 1963.

10. Rideout, S. P.; Ondrejcin, R. S.; Louthan, M. R., Jr.; and Rawl, D. E.: The Role of Moisture and Hydrogen in Hot-Salt Cracking of Titanium Alloys. Fundamental Aspects of Stress Corrosion Cracking. R. W. Staehle, A. J. Forty, and D. van Rooyen, eds., Nat. Assoc. Corrosion Eng., 1969, pp. 650-661.

11. Ripling, E. J.; Kirchner, R. L.; O'Shea, R. P.; and Lingwall, R. G.: Elevated Temperature Stress Corrosion of High Strength Sheet Materials in the Presence of Stress Concentrations. Materials Research Lab., Inc. (NASA CR-69851), Nov. 1965.

12. Cotton, F. Albert; and Wilkinson, G.: Advanced Inorganic Chemistry. Interscience Publ., 1962.

13. Martin, George: Investigation of Long-Term Exposure Effects Under Stress of Two Titanium Structural Alloys. Stress-Corrosion Cracking of Titanium. Spec. Tech. Publ. No. 397, ASTM, 1966, pp. 95-121.

14. Heimerl, G. J.; Braski, D. N.; Royster, D. M.; and Dexter, H. B.: Salt Stress Corrosion of Ti-8Al-1Mo-1V Alloy Sheet at Elevated Temperatures. Stress-Corrosion Cracking of Titanium. Spec. Tech. Publ. No. 397, ASTM, 1966, pp. 194-214.

15. Brauer, George, ed.: Handbook on Preparative Inorganic Chemistry. Second ed., Academic Press, 1963, p. 1199.

16. Stone, L. H.; and Freedman, A. H.: Cyclic Hot-Salt Stress Corrosion of Titanium Alloys. Rep. NOR-67-151, Northrop Corp. (AFML-TR-67-289, AD-825239), Sept. 1967.

17. Fisher, James R.; and Barnes, H. L.: The Ion-Product Constant of Water to 350°. J. Phys. Chem., vol. 76, no. 1, Jan. 6, 1972, pp. 90-99.

18. Petersen, V. C.; and Bomberger, H. B.: The Mechanism of Salt Attack on Titanium Alloys. Stress-Corrosion Cracking of Titanium. Spec. Tech. Publ. No. 397, ASTM, 1966, pp. 80-94.

19. Gray, Hugh R.: Role of Hydrogen in Hot-Salt Stress-Corrosion of a Titanium Alloy. NASA TN D-6188, 1971.

20. Oriani, R. A.: Hydrogen in Metals. Fundamental Aspects of Stress Corrosion Cracking. R. W. Staehle, A. J. Forty, and D. van Rooyen, eds., Nat. Assoc. Corrosion Eng., 1969, pp. 32-50.

21. Oriani, R. A.: Consequence of Strain Induced Electric Field at Roots of Cracks. Scripta Metallurg., vol. 5, no. 8, Aug. 1971, pp. 697-700.

22. Gray, Hugh R.: Ion and Laser Microprobes Applied to the Measurement of Corrosion-Produced Hydrogen on a Microscopic Scale. NASA TN D-6521, 1971. (Also available in Corrosion, vol. 28, no. 2, Feb. 1972, pp. 47-54.)

23. Gross, Bernard; and Mendelson, Alexander: Plane Elastostatic Analysis of V-Notched Plates. NASA TN D-6040, 1970.

24. Gray, Hugh R.: Hot-Salt Stress-Corrosion of Titanium Alloys as Related to Turbine Engine Operation. Paper presented at Second International Conference on Titanium sponsored by the Metallurgical Society and the American Society for Metals (Cambridge, Massachusetts), May 1972.

25. Piper, D. E.; and Fager, D. N.: The Relative Stress-Corrosion Susceptibility of Titanium Alloys in the Presence of Hot Salt. Stress-Corrosion Cracking of Titanium. Spec. Tech. Publ. No. 397, ASTM, 1966, pp. 31-52.

26. McBreen, J.; and Genshaw, M. A.: The Electrochemical Introduction of Hydrogen into Metals. Fundamental Aspects of Stress Corrosion Cracking. R. W. Staehle, A. J. Forty, and D. van Rooyen, eds., Nat. Assoc. Corrosion Eng., 1969, pp. 51-63.

27. Gray, Hugh R.: Relative Susceptibilities of Titanium Alloys to Hot-Salt Stress-Corrosion. NASA TN D-6498, 1971.

28. Rideout, S. P.: The Initiation of Hot-Salt Stress Corrosion Cracking of Titanium Alloys. Applications Related Phenomena in Titanium Alloys. Spec. Tech. Publ. No. 432, ASTM, 1968, pp. 205-217.

29. Donachie, M. J., Jr.; Danesi, W. P.; and Pinkowish, A. A.: Effects of Salt Atmosphere on Crack Sensitivity of Commercial Titanium Alloys at 600° to 900° F. Stress-Corrosion Cracking of Titanium. Spec. Tech. Publ. No. 397, ASTM, 1966, pp. 179-193.

30. Heslop, R. B.; and Robinson, P. L.: Inorganic Chemistry. Elsevier Publ. Co., 1960, pp. 263, 427.

31. Boyd, W. K.: Stress Corrosion Cracking of Titanium and Its Alloys. Fundamental Aspects of Stress Corrosion Cracking. R. W. Staehle, A. J. Forty, and D. van Rooyen, eds., Nat. Assoc. Corrosion Eng., 1969, pp. 593-604.

32. Petersen, V. C.: Hot-Salt Stress-Corrosion of Titanium. J. Metals, vol. 23, no. 4, Apr. 1971, pp. 40-47.

33. Weast, Robert C., ed.: Handbook of Chemistry and Physics. 51st ed., Chemical Rubber Co., 1970.

34. Mellor, J. W.: A Comprehensive Treatise on Inorganic and Theoretical Chemistry. Vol. 5. Longmans, Green and Co., 1924, p. 319.

35. Ondrejcin, R. S.; Selby, C. L.; and Rideout, S. P.: Role of Chloride in Hot Salt Stress-Corrosion Cracking of Titanium-Aluminum Alloys. Rep. DP(NASA)-1118, E. I. Du Pont de Nemours & Co. (NASA CR-87817), July 1967, p. 15.

36. Latimer, Wendell M.: Oxidation Potentials. Second ed., Prentice-Hall, Inc., 1952, p. 339.

TABLE I. - SUPPLIER'S ANALYSIS OF
COMMERCIAL TITANIUM ALLOY
Ti-811 SHEET STOCK

Element	Wt. %
Al	7.8
Mo	1.1
V	1.1
Fe	.09
C	.032
N	.013
H	.0055

TABLE II. - TENSILE PROPERTIES OF COLD
ROLLED SHEET MATERIAL

Temperature		Ultimate strength		Rupture strength for 24-hour exposure	
K	$^\circ$F	MN/m^2	ksi	MN/m^2	ksi
Titanium alloy Ti-811					
625	666	993	144	985	143
650	710	972	141	938	136
700	800	924	134	876	127
Unalloyed titanium					
350	170	758	110	683	99
650	710	393	57	379	55

TABLE III. - ANALYSES OF GASES USED FOR FURNACE ATMOSPHERES

Gas	Impurity, ppm				
	H_2	H_2O	O_2	Ar	N_2
Nitrogen	220	5	5	180	Balance
Oxygen	120	10	Balance	2980	34

TABLE IV. - EFFECT OF CATHODE HYDROGEN ION CONCENTRATION ON HALF-CELL POTENTIALS OF CORROSION PROCESS AT 650 K (710° F)

	Reaction	Surface additive					
		Neutral		Acidic		Basic	
		pH	emf, V	pH	emf, V	pH	emf, V
Anode	$Ti + 2H_2O = TiO_2 + 4H^+ + 4e^-$	6	1.8	6	1.8	6	1.8
Cathode	$O_2 + 4H^+ + 4e^- = 2H_2O$	6	0.3	1	1.1	11	-0.4
Cell	$Ti + O_2 = TiO_2$		2.1		2.9		1.4

TABLE V. - STRESS-CORROSION RUPTURE DATA FOR TITANIUM ALLOY Ti-811 SPECIMENS EXPOSED TO NITROGEN AND OXYGEN AT VARIOUS TEMPERATURES

(a) Exposure temperature, 625 K (665° F)

Specimen	Exposure data		Tensile data		
	Moisture content, ppm	Stress, %RS (a)	Fracture stress		Elongation, percent
			MN/m^2	ksi	
		Nitrogen			
2407-2	$<10^{-4}$	51	986	143	9.3
2408-2	↓	60	1060	154	8.1
2408-1		68	980	142	8.4
2505-2		73	993	144	7.7
2505-1		86	1090	158	5.9
2401-1	$>10^4$	68	945	137	9.5
2403-2	$>10^4$	77	903	131	8.8
2403-1	$>10^4$	86	938	136	9.4
		Oxygen			
2507-2	$<10^{-4}$	73	1060	153	5.8
2410-1	$<10^{-4}$	77	980	142	7.6
2507-1	$<10^{-4}$	86	993	144	6.3
2729-2	10	68	938	136	9.2
2729-1	10	80	1010	146	8.1
2323-2	$>10^4$	51	980	142	9.2
2323-1	↓	60	993	144	8.5
2324-2		64	1160	168	1.7
2319-1		68	1120	162	.9
2324-1		73	1090	158	2.4

[a] Percent rupture stress.

TABLE V. - Continued. STRESS-CORROSION RUPTURE DATA FOR TITANIUM ALLOY Ti-811 SPECIMENS EXPOSED TO NITROGEN AND OXYGEN AT VARIOUS TEMPERATURES

(b) Exposure temperature, 650 K (710° F)

Specimen	Exposure data		Tensile data		
	Moisture content, ppm	Stress, %RS (a)	Fracture stress		Elongation, percent
			MN/m^2	ksi	
			Nitrogen		
1704-2	$<10^{-4}$	13	1080	156	6.5
1704-1		22	1200	174	2.2
1705-2		26	1190	172	2.3
1705-1		30	834	121	0
0827-1		43	627	91	0
0916-1		52	545	79	0
2027-2	10	17	1080	157	6.4
1418-1		26	1030	150	6.7
1418-2		35	1090	158	6.6
1416-1		39	717	104	0
1920-2	10^3	30	1190	172	2.2
1920-1		39	1180	171	2.7
1719-2		43	1030	150	6.9
2116-2		47	910	132	10.7
1218-2		52	1180	171	2.4
1217-2		61	1160	168	.9
2017-1	$>10^4$	17	1080	157	6.7
2117-1		39	993	144	8.3
2121-1		43	1130	164	3.4
1930-1		47	1190	173	2.1
2122-2		52	1170	170	2.1
2122-1		61	1160	168	.3
			Oxygen		
1714-2	$<10^{-4}$	9	1180	171	2.0
1714-1		17	1150	166	1.0
1713-2		26	1020	148	0
1713-1		35	579	84	0
1711-2		52	531	77	0
2026-2	10	17	1060	153	7.2
2026-1		26	1080	157	7.5
1718-2		35	848	123	0
1718-1		52	745	108	0
2114-2	10^3	22	1090	158	7.2
2108-2		30	1140	165	5.7
2024-2		39	1100	160	6.4
2114-1		47	1090	158	0
1209-2		52	1010	146	0
1208-2		55	1090	158	0
2004-2	$>10^4$	26	1160	168	2.9
2010-2		30	1170	169	3.3
1012-2		35	1160	168	4.7
2010-1		39	1140	165	3.9
1012-1		43	1120	162	0
2124-1		52	(b)	---	----

[a] Percent rupture stress.

[b] Specimen broke in exposure rig.

TABLE V. - Concluded. STRESS-CORROSION RUPTURE DATA FOR TITANIUM ALLOY Ti-811 SPECIMENS EXPOSED TO NITROGEN AND OXYGEN AT VARIOUS TEMPERATURES

(c) Exposure temperature, 700 K (800° F)

Specimen	Exposure data		Tensile data		
	Moisture content, ppm	Stress, %RS (a)	Fracture stress		Elongation, percent
			MN/m^2	ksi	
		Nitrogen			
2222-2	$<10^{-4}$	23	945	137	9.4
2226-2		27	993	144	9.7
2226-1		27	(b)	---	---
2222-1		36	(b)	---	---
2219-2	10	23	1010	146	6.1
2220-2		27	993	144	9.5
2220-1		31	696	101	0
2219-1		36	496	72	0
2214-2	10^3	27	1000	145	9.4
2215-2		31	669	97	0
2214-1		36	869	126	0
2215-1		40	814	118	0
2206-2	$>10^4$	14	1020	148	9.2
2208-2		18	1050	152	7.6
2208-1		23	1060	154	9.2
2206-1		27	1120	162	1.8
		Oxygen			
2229-2	$<10^{-4}$	23	993	144	9.7
2229-1	$<10^{-4}$	36	(b)	---	---
2304-2	10	23	1040	151	8.2
2305-2		27	951	138	9.8
2305-1		27	1050	152	.2
2304-1		36	979	142	0
2312-2	10^3	14	993	144	7.4
2312-1		18	1010	147	8.1
2309-2		23	1030	149	1.5
2309-1		36	903	131	0
2316-2	$>10^4$	23	972	141	8.9
2317-2		27	1130	164	.5
2317-1		31	993	144	.1
2316-1		36	607	88	0

[a] Percent rupture stress.

[b] Specimen broke in exposure rig.

TABLE VI. - STRESS-CORROSION RUPTURE DATA FOR TITANIUM ALLOY Ti-811 SPECIMENS EXPOSED AT 650 K (710° F) TO OXYGEN WITH A MOISTURE CONTENT OF 10 ppm

Specimen	Exposure data		Tensile data		
	Additive	Stress, %RS (a)	Fracture stress		Elongation, percent
			MN/m^2	ksi	
2822-2	Control	26	924	134	10.2
1718-2	Control	35	848	123	0
2701-2	10 percent CO_2	17	1050	152	5.1
2704-1	10 percent CO_2	22	1130	164	4.7
2701-1	10 percent CO_2	26	779	113	0
3203-2	NaOH in methanol	68	993	144	9.2
3203-1	NaOH in methanol	78	938	136	8.7

[a] Percent rupture stress.

TABLE VII. - EFFECT OF IMPRESSED POTENTIAL ON RUPTURE DATA FOR TITANIUM ALLOY Ti-811 SPECIMENS EXPOSED AT 650 K (710° F) TO OXYGEN WITH A MOISTURE CONTENT GREATER THAN 10^4 ppm

Specimen	Exposure data		Tensile data		
	Impressed potential, V	Stress, %RS (a)	Fracture stress		Elongation, percent
			MN/m^2	ksi	
2004-2	Control	26	1160	168	2.9
3306-1	36	26	690	100	0

[a] Percent rupture stress.

TABLE VIII. - STRESS-CORROSION RUPTURE DATA FOR UNALLOYED TITANIUM SPECIMENS EXPOSED AT 650 K (710° F) TO OXYGEN

Specimen	Exposure data		Tensile data		
	Moisture content, ppm	Stress, %RS (a)	Fracture stress		Elongation, percent
			MN/m^2	ksi	
2722-2	10	63	655	95	19.1
2722-1	10	84	634	92	20.4

[a] Percent rupture stress.

TABLE IX. - EFFECT OF IMPRESSED POTENTIAL ON RUPTURE DATA FOR UNALLOYED TITANIUM SPECIMENS EXPOSED AT 350 K (170° F) TO OXYGEN (WITH A MOISTURE CONTENT $>10^4$ ppm) WITH LITHIUM CHLORIDE SALT

Specimen	Exposure data		Tensile data		
	Impressed potential, V	Stress, %RS (a)	Fracture stress		Elongation, percent
			MN/m^2	ksi	
3323-2	Control	75	772	112	17.5
3323-1	72	75	814	118	3.2

[a] Percent rupture stress.

TABLE X. - ELECTRODE HALF-CELL POTENTIALS FOR ELECTROCHEMICAL STRESS-CORROSION PROCESSES IN 10^{-6} M SOLUTION AT 650 K (710° F)

	Reaction	Potential
Aluminum anode	$2Al + 3H_2O = 6H^+ + Al_2O_3 + 6e^-$	2.3
Titanium cathode	$3/2\ O_2 + 6H^+ + 6e^- = 3H_2O$	.3
Cell	$2Al + 3/2\ O_2 = Al_2O_3$	2.6
Magnesium anode	$Mg + 2Cl^- = MgCl_2 + 2e^-$	0.9
Titanium cathode	$1/2\ O_2 + 2H^+ + 2e^- = H_2O$	.3
Cell	$Mg + 1/2\ O_2 + 2HCl = MgCl_2 + H_2O$	1.2
Titanium anode	$Ti + 2H_2O = 4H^+ + TiO_2 + 4e^-$	1.8
Palladium cathode	$O_2 + 4H^+ + 4e^- = 2H_2O$	.3
Cell	$Ti + O_2 = TiO_2$	2.1

TABLE XI. - STRESS-CORROSION RUPTURE DATA FOR TITANIUM ALLOY Ti-811 SPECIMENS EXPOSED AT 650 K (710° F) TO OXYGEN WITH A MOISTURE CONTENT OF 10 ppm

Specimen	Exposure data		Tensile data		
	Coating	Stress, %RS (a)	Fracture stress		Elongation, percent
			MN/m^2	ksi	
2822-2	Control	26	924	134	10.2
1718-2	Control	35	848	123	0
2826-2	Palladium	35	1100	160	4.7
2828-2	Palladium	43	752	109	0
2819-1	Aluminum	26	703	102	0
2819-2	Aluminum	35	1140	166	.3
2826-1	Magnesium	35	938	136	9.3
2826-2	Magnesium	43	965	140	10.4
2925-2	Magnesium	52	1170	170	5.9
		69	1110	161	6.7

[a] Percent rupture stress.

NATIONAL AERONAUTICS AND SPACE ADMISTRATION
WASHINGTON, D.C. 20546

OFFICIAL BUSINESS
PENALTY FOR PRIVATE USE $300

FIRST CLASS MAIL

POSTAGE AND FEES PAID
NATIONAL AERONAUTICS AND
SPACE ADMINISTRATION

U.S.MAIL

```
020 001 C1 U  17 720414 S00903DS
DEPT OF THE AIR FORCE
AF WEAPONS LAB (AFSC)
TECH LIBRARY/WLOL/
ATTN: E LOU BOWMAN, CHIEF
KIRTLAND AFB NM 87117
```

POSTMASTER: If Undeliverable (Section 158 Postal Manual) Do Not Return

---

> *"The aeronautical and space activities of the United States shall be conducted so as to contribute . . . to the expansion of human knowledge of phenomena in the atmosphere and space. The Administration shall provide for the widest practicable and appropriate dissemination of information concerning its activities and the results thereof."*
>
> —NATIONAL AERONAUTICS AND SPACE ACT OF 1958

NASA SCIENTIFIC AND TECHNICAL PUBLICATIONS

TECHNICAL REPORTS: Scientific and technical information considered important, complete, and a lasting contribution to existing knowledge.

TECHNICAL NOTES: Information less broad in scope but nevertheless of importance as a contribution to existing knowledge.

TECHNICAL MEMORANDUMS: Information receiving limited distribution because of preliminary data, security classification, or other reasons.

CONTRACTOR REPORTS: Scientific and technical information generated under a NASA contract or grant and considered an important contribution to existing knowledge.

TECHNICAL TRANSLATIONS: Information published in a foreign language considered to merit NASA distribution in English.

SPECIAL PUBLICATIONS: Information derived from or of value to NASA activities. Publications include conference proceedings, monographs, data compilations, handbooks, sourcebooks, and special bibliographies.

TECHNOLOGY UTILIZATION PUBLICATIONS: Information on technology used by NASA that may be of particular interest in commercial and other non-aerospace applications. Publications include Tech Briefs, Technology Utilization Reports and Technology Surveys.

Details on the availability of these publications may be obtained from:

SCIENTIFIC AND TECHNICAL INFORMATION OFFICE

NATIONAL AERONAUTICS AND SPACE ADMINISTRATION
Washington, D.C. 20546